Journal of Hydrology 557 (2018) 67–82

Contents lists available at ScienceDirect

Journal of Hydrology

journal homepage: www.elsevier.com/locate/jhydrol

Research papers

Variability of onset and retreat of the rainy season in mainland China and associations with atmospheric circulation and sea surface temperature

Qing Cao [a], Zhenchun Hao [a,b,*], Quanxi Shao [c], Jie Hao [d], Tsring Nyima [e]

[a] State Key Laboratory of Hydrology Water Resources and Hydraulic Engineering, Hohai University, Nanjing 210098, China
[b] National Cooperative Innovation Center for Water Safety & Hydro-Science, Hohai University, Nanjing 210098, China
[c] CSIRO DATA61, Private Bag 5, Wembley, WA 6913, Australia
[d] Nanjing Hydraulic Research Institute, Nanjing 210098, China
[e] Investigation Bureau of Hydrology and Water Resources in Ali of Tibet Autonomous Region, Tibet 859000, China

ARTICLE INFO

Article history:
Received 4 August 2017
Received in revised form 18 November 2017
Accepted 7 December 2017
Available online 9 December 2017
This manuscript was handled by G. Syme, Editor-in-Chief, with the assistance of Saeid Eslamian, Associate Editor

Keywords:
Rainy season
Onset
Retreat
Moving *t*-test
Atmospheric circulation
SST

ABSTRACT

Precipitation plays an important role in both environment and human society and is a significant factor in many scientific researches such as water resources, agriculture and climate impact studies. The onset and retreat of rainy season are useful features to understand the variability of precipitation under the influence of climate change. In this study, the characteristics of onset and retreat in mainland China are investigated. The multi-scale moving *t*-test was applied to determine rainy season and K-means cluster analysis was used to divide China into sub-regions to better investigate rainy season features. The possible linkage of changing characteristics of onset and retreat to climate factors were also explored. Results show that: (1) the onset started from middle March in the southeast of China to early June in the northwest and rainy season ended earliest in the northwest and southeast while the central China had the latest retreat; (2) Delayed onset and advanced retreat over time were observed in many parts of China, together with overall stable or increased rainy-season precipitation, would likely lead to higher probability of flooding; (3) The onset (retreat) was associated with the increased (decreased) number of cyclones in eastern China and anticyclone near the South China Sea. Delayed onset, and advanced retreat were likely related to cold and warm sea surface temperature (SST) in the conventional El Niño-Southern Oscillation (ENSO) regions, respectively. These results suggest that predictability of rainy season can be improved through the atmospheric circulation and SST, and help water resources management and agricultural planning.

1. Introduction

Precipitation is one of the most important variable responding to climate change, which has attracted urgent attention worldwide. Various aspects of precipitation have been investigated, such as seasonality and extremes (Ashok et al., 2009; Feng et al., 2011; Ratnam et al., 2011; Su et al., 2005; Taschetto and England, 2009; Tedeschi et al., 2013; Wang et al., 2013; Zhang et al., 2016). Unfortunately, characteristics of rainy season are less considered but are of vital significance to influence socio-economy. Reliable prediction of the onset of rainy season will reduce the risk of improper planting/sowing time, and assist on-time preparation of farmlands (Liebmann and Marengo, 2001; Marteau et al., 2011; Omotosho et al., 2000). A good knowledge of the retreat of rainy season is useful for the selection of crop varieties and has significant impact to ecosystem (Liebmann et al., 2007). Rainy-season precipitation will also provide certain predictability for flood occurrence and be helpful to flood monitoring. The variability of onset and retreat of rainy season and the total precipitation amount during rainy season are also direct indications for climate change and provide good scientific support to socio-economic development and climate change research.

For a large region, like China as a whole, rainy season varies substantially in both space and time. Previous researches have been limited to the analysis of the total precipitation during rainy season and ignored the onset and retreat. Many works were focused on regional scales (e.g., northwestern China, the Yangtze river basin and the coastal areas) (Chen et al., 2007; Gemmer

* Corresponding author at: State Key Laboratory of Hydrology Water Resources and Hydraulic Engineering, Hohai University, Nanjing 210098, China.
E-mail address: zhenchunhao@163.com (Z. Hao).

https://doi.org/10.1016/j.jhydrol.2017.12.026
0022-1694/

et al., 2011; Su et al., 2005; Wang et al., 2013; Zhang et al., 2009), without the consideration of spatial heterogeneity, which is an important factor for the continental scale. Hence, the investigation of rainy season features variability, such as the onset and retreat, is necessary in China at the continental scale, in order to gain insight of rainfall characteristics.

There has not been a consensus agreement regarding to the determination of rainy season, due to irregularities in rainfall distribution in both space and time. In literature, the determination of rainy season can be based on rainfall data, temperature, deep convection, monsoon or combination of several indices (Cook and Heerdegen, 2001; Gan et al., 2004, 2005; Goswami and Xavier, 2005; Janowiak and Xie, 2003; Liebmann et al., 2007; Qian and Lee, 2000; Reason et al., 2005). The majority of research used threshold values of a given index (or indices) to determine the onset and retreat, which is somewhat subjective. Therefore, a data originated objective method, called the multi-scale moving *t*-test, was used in this study to detect rainy season. The onset and retreat defined by this method does not require an ad-hoc threshold as in most traditional definitions. There are also some other statistically based methods used to detect the rainy season, such as the optimal segmentation method of ordered sample, which can further divide the rainy season into several sub-periods. Nonetheless, this paper is just focused on the onset and retreat rather than the detailed types of rainy season. Therefore, the multi-scale moving *t*-test is better for this research over others based on literature.

In order to understand the driving factors or the causes of the change in rainy season, the correlations with monsoon and sea surface temperature (SST) are evaluated as they are the main factors influencing rainy season characteristics of China (Deng and Wang, 2002; Ding and Chan, 2005; Liu and Ding, 2008; Lu, 2005; Wang and LinHo, 2002; Wang et al., 2004, 2002; Yang and Lau, 2004; Zhao et al., 2010). From a meteorological perspective, the onset and retreat reflect the changes in an atmospheric heat source, whose addition or subtraction can alter large-scale and regional circulation (Figueroa et al., 1995; Lenters and Cook, 1997). SST is important for developing and maintaining atmospheric circulations (Fan et al., 2013). Previous research have found that rainy-season precipitation in China shows good relation to SST (e.g., Deng and Wang (2002)). As a consequence, it is meaningful to investigate signals of rainy season characteristics through monsoon and lag period SST.

In this paper, we will explore features of rainy season in mainland China at the continental scale. The homogeneous regions will be determined based on rainy season characteristics including the onset, retreat and rainy-season precipitation. The interannual variability of rainy season within individual homogeneous regions will be further investigated. We will also explore the possible correlation of the onset and retreat with monsoon and SST to understand the signals of variability of the onset and retreat. This study is of importance for helping us to provide a certain predictability to flooding occurrence and of great significance to understand hydrological cycle and water resource management under climate change in China.

The paper is organized as below. The study area and data are described in Section 2, followed by the methodology in Section 3. Results and discussion regarding interannual features of rainy season and their underlying correlation to monsoon and SST are presented in Section 4. The paper is concluded by a summary of the findings in Section 5.

2. Study area and data

China (Fig. 1), located in middle latitude in the Northern Hemisphere, has variable climate (i.e., the monsoon climate, the continental climate, the mountain plateau climate). China is prone to flood and drought occurrence in different regions and climate change is taken as one of the leading drivers for precipitation changes in the country.

Daily precipitation data from 1960 to 2015 at 536 meteorological stations in mainland China were used in this study. The data were obtained from the China Meteorological Data Sharing Service System (http://data.cma.cn/data/detail/dataCode/SURF_CLI_CHN_MUL_DAY_V3.0.html) and data quality were controlled based on national standards. Meteorological stations, which have at least 50 years complete data, were selected to describe rainy season characteristics. Locations of precipitation stations used in this study are presented in Fig. 1, with more observation stations in southeastern China as compared to northwestern regions. Therefore, we applied kriging interpolation method to induce a resolution of $0.2^\circ \times 0.2^\circ$.

NCEP-NCAR reanalysis data (https://www.esrl.noaa.gov/psd/data/gridded/data.ncep.reanalysis.html) were used to explore relationship of rainy season and monsoon, where 850hpa vector winds data were selected (Kalnay et al., 1996). NOAA extended reconstructed SST data (https://www.ncdc.noaa.gov/data-access/marineocean-data/extended-reconstructed-sea-surface-temperature-ersst-v4) were used to consider correlation between rainy season and SST (Smith and Reynolds, 2004).

3. Methodology

The methods used in this paper includes the multi-scale moving *t*-test (Section 3.1) to determine the onsets and retreats of rainy season, K-means cluster analysis method (Section 3.2) to divide the mainland China into several obtain homogeneous sub-regions according to rainy season features (i.e., the onset, retreat and precipitation), trend analysis and Pettitt test for abrupt point analysis (Section 3.3) of rainy season characteristics in individual sub-regions, and Pearson coefficient correlations (Section 3.4) to explain the underlying relationship between rainy season characteristics and SST.

3.1. Determination of onset and retreat

The multi-scale moving *t*-test method was applied to determine the onset and retreat by detecting the most significant change between two subsamples before and after the abruption point with equal sample sizes n, where n is the length of the subsample, (n = 30, 31,. . ., 182 or 183). Here 182 or 183 corresponds to half the value of length of one year 365 or 366). Theoretically, the length of subsamples ranged from 1 to 182/183. Nonetheless, for the onset or retreat of rainy season, it is not reasonable if the length of the subsample is just one day or several days when the mutation point is prominent. Hence, the length of the subsample is limited from 30 to 182/183. The multi-scale abruption points can be detected as (Fraedrich et al., 1997):

$$t(n,i) = (\bar{x}_{i2} - \bar{x}_{i1})n^{1/2}\left(s_{i2}^2 + s_{i1}^2\right)^{-1/2}, \quad (1)$$

where $\bar{x}_{i1}$ and $\bar{x}_{i2}$ defined as:

$$\bar{x}_{i1} = \sum_{j=i-n}^{i-1} x_j/n; s_{i1}^2 = \sum_{j=i-n}^{i-1}(x_j - \bar{x}_{i1})^2/(n-1), \quad (2)$$

$$\bar{x}_{i2} = \sum_{j=i}^{i+n-1} x_j/n; s_{i2}^2 = \sum_{j=i}^{i+n-1}(x_j - \bar{x}_{i2})^2/(n-1), \quad (3)$$

and x_i is daily precipitation for Julian day i for one station within one year. $\bar{x}_{i1}$ and $\bar{x}_{i2}$ are averaged values of subsamples before and after the Julian day i, respectively.

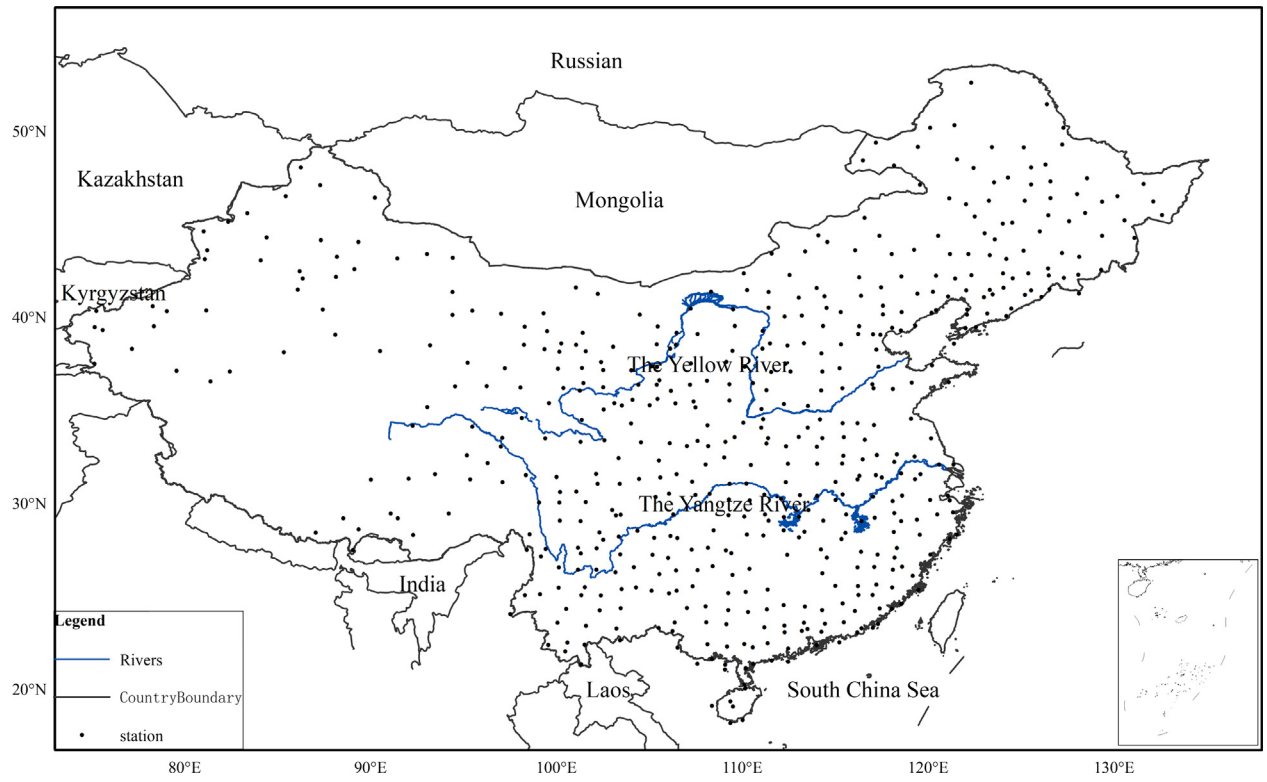

Fig. 1. The distribution of meteorological stations used in this study.

The t-value was normalized by the 0.01 test value showing in Eq. (4), which is equivalent to the results of the Mann-Kendall test at 0.05 significance level.

$$t_r(n,i) = t(n,i)/t_{0.01}(n), \tag{4}$$

where $t_r(n,i)$ can be considered as the threshold to detect abruption points. $t_r(n,i) > 1.0$ is an increasing trend while $t_r(n,i) < 1.0$ is a decreasing trend. The onset of rainy season was defined as the abruption point corresponding to a maximum $t_r(n,i)$ value, where precipitation changes from a smaller to a larger value. Likewise, the retreat is defined as the changing point corresponding to a minimum $t_r(n,i)$ value.

Taking daily precipitation data in one year at one station, which is selected from region 1 classified in Fig. 4, as an example to present the determination of the onset and retreat (Fig. 2a). The yellow greenish lines denote positive $t_r(n,i)$ values, and the blue lines denote negative values. Fig. 2a reveals that the maximum value of $t_r(n,i)$ is 1.35, when the corresponding Julian day is 106 and the corresponding timescale is 96. It means that the onset date of rainy season is Julian day 106, which shows the most conspicuous abruption in the timescale of 96 days. Similarly, the retreat date of rainy season is Julian day 260.

3.2. K-means cluster analysis for regionalization

It is necessary to divide China into sub-regions to explore rainy season features, due to the heterogeneity of Chinese rainy season characteristics. Previous studies have used administration or climatic zones as the criteria to determine homogeneous sub-regions. However, they are not statistically sound, because they do not directly reflect rainy season characteristics from observations. In this study, the K-means clustering with factors of the onset, retreat of rainy season and total precipitation during rainy season is used to determine the homogeneous sub-regions due to high efficiency in dealing with large amount of data.

K-means cluster algorithm aims to find a partition so that the squared error between empirical mean of a cluster and points in the cluster is minimized. The squared error is defined as (Jain, 2010):

$$J(C_k) = \sum_{x_i \in C_k} \|x_i - \mu_k^2\|, \tag{5}$$

where x_i are parameters (i.e., mean onset, retreat and rainy-season precipitation for the period of 1960–2015) in i_{th} station, $X = \{x_i\}, i = 1, \ldots, n$, is clustered into a set of K clusters. μ_k is the mean value of cluster C_k, $J(C_k)$ the squared error of cluster C_k, where $C = \{C_k\}, k = 1, \ldots, K$.

The objective of K-means cluster analysis is to minimize the sum of squared error in all K clusters.

$$J(C) = \sum_{k=1}^{K} \sum_{x_i \in C_k} \|x_i - \mu_k^2\|, \tag{6}$$

In this study, K is equal to 5 considering the number of administration and climate zones in China.

3.3. Pettitt test for change point analysis

Within the homogeneous sub-regions, the features of rainy season (i.e., the onset, retreat and total precipitation) evaluated over time. Pettit test was applied to detect a single change-point in interannual onset/retreat/precipitation series in order to evaluate the influence of climate change on rainy season. More than one change points can be detected if other methods such as the Mann-Kendall test are used. The reason why choosing the Pettitt test is that we want to detect the most prominent change point.

Pettitt test was used to detect a single abruption point in interannual onset/retreat/precipitation series X_i, i = 1, 2, …, 56, where X_i

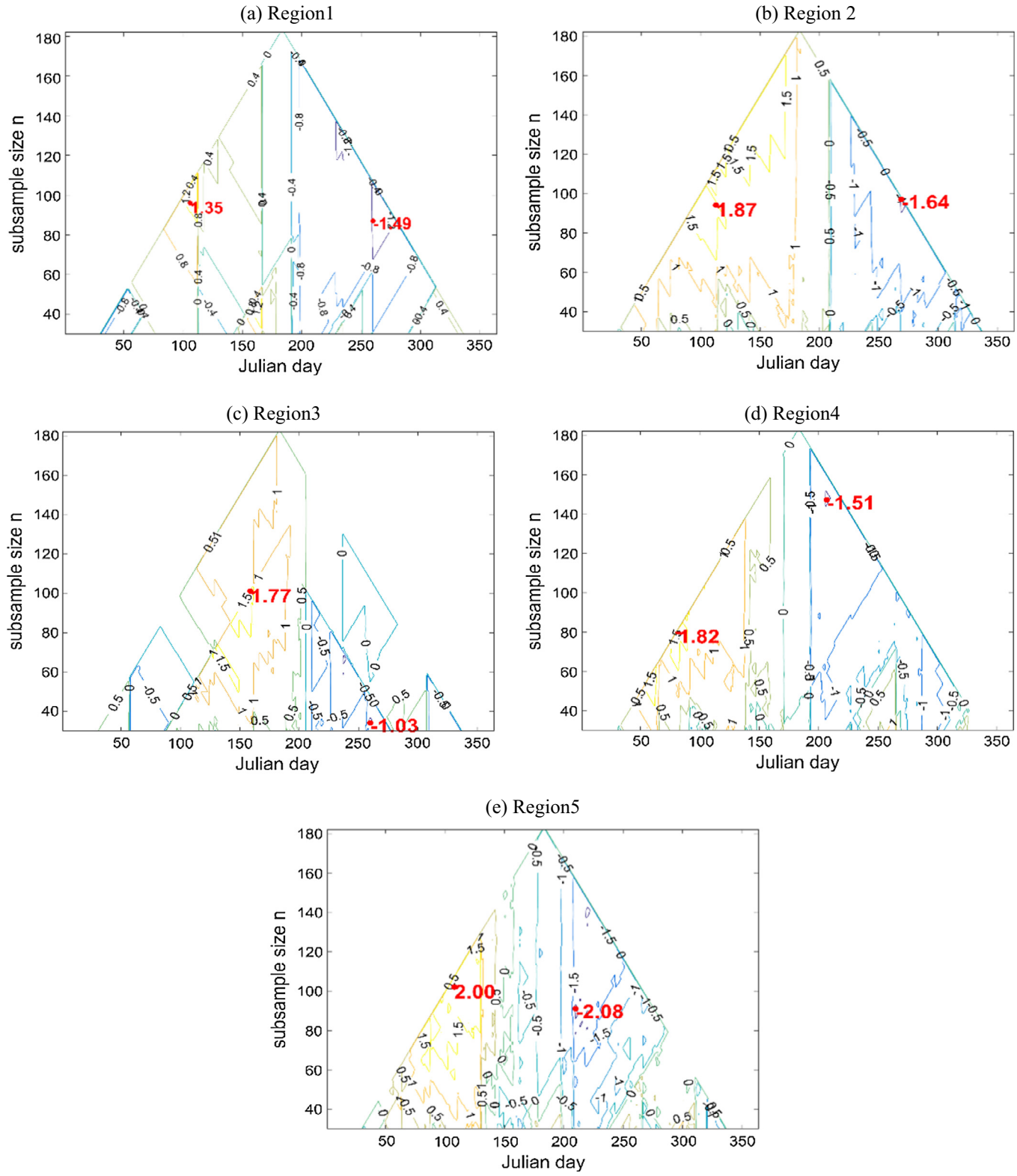

Fig. 2. The determination of rainy season in meteorological stations by multi-scale moving *t*-test. Fig. 2a represents that the meteorological station is selected from region1 classified in Fig. 4. Similarly, Fig. 2b-e represents that the meteorological station is selected from region2-5, respectively.

represents the mean onset/retreat/precipitation of stations in one sub-region and for i_{th} year. The non-parametric statistic is defined as follows (Pettitt, 1979):

$$K_T = max|U_{t,T}|, \tag{7}$$

where

$$U_{t,T} = \sum_{i=1}^{t}\sum_{j=t+1}^{T} sgn(X_i - X_j), \tag{8}$$

K_T can be considered as the abruption point of series and the result is meaningful when K_T <0.5. The parameter P is applied to judge the significant level of the abruption point, which is defined as:

$$P = 2exp\left[\frac{-6K_T^2}{n^3 + n^2}\right], \quad (9)$$

and n = 56 in this study. When P is <0.05, it means that the change point is significant at the significance level of 0.05.

3.4. Correlation evaluation between onset, retreat and SST

The Pearson liner correlation coefficients between rainy season characteristics and SST were evaluated. The Pearson liner correlation coefficient r can be calculated as (Pearson, 1895):

$$r = \frac{\sum_{i=1}^{56}\sum_{j=2}^{11}\sum_{k=j-z}^{j-z-9}(x_{ij} - \bar{x})(y_{ik} - \bar{y})}{\sqrt{\sum_{i=1}^{56}\sum_{j=2}^{11}(x_{ij} - \bar{x})^2 \sum_{i=1}^{56}\sum_{k=j-z}^{j-z-9}(y_{ik} - \bar{y})^2}}, \quad (10)$$

x_{ij} represents mean onset/retreat at $j_{th} - 1$, j_{th}, $j_{th} + 1$ month in i_{th} year and for one sub-region and $x_{i2} = x_{i3} = \ldots = x_{i11}$; $\bar{x}$ the mean onset/retreat in one sub-region for the period of 1960–2015; y_{ik} represents mean SST at $k_{th} - 1$, k_{th}, $k_{th} + 1$ month in i_{th} year; z represents the value of months that SST lagged onset/ retreat, and z ranges between 1 and 12,because we want to evaluate lag-correlation between rainy season characteristics and preceding 1–12 months SST; $\bar{y}$ the mean SST for the period of 1960–2015 or 1959–2014.

4. Results and discussion

4.1. Regionalization of mainland China

The average onset dates of rainy season during 1960–2015 in China varied from Julian day 75–155 (Fig. 3a). The onset progressed northwestwards from mid-March in coastal regions in the southeast to the beginning of June in the northwest. The central and northeastern regions of China had median onset, ranging from mid-April to mid-May. Different methods to define summer monsoon onset dates related to the rainy season have been presented in previous studies. For example, Wang and LinHo (2002) designed a compound rainfall variable, which can synthesize three characteristics (i.e., the total amount of summer rainfall, the annual range of rainfall and the seasonal distribution of rainfall), to determine the onset of rainy season. Their results show that the Asian monsoon rainy season begins over the South China Sea and then advances northwestwards, which is in accordance with our research.

Rainy season ended earliest in the southeast as well (Fig. 3b), with the retreat occurring in late July. Overall, the retreat progressed from the coastal areas to central China (100°E-110°E, 20°N-35°N) and shrank from the central regions to the northwest, with rainy season ending in September and October in Central China and late July and August in the northwest. The distribution of precipitation is similar to the onset (Fig. 3c), with rainy-season precipitation shrinking from southeast (1500–1800 mm) to northwest (2–300 mm).

In summary, rainy season started and ended earliest in coastal regions and had largest amount of rainy-season precipitation. Central China had median values of onset and precipitation, with latest retreat. Northwestern China had smallest precipitation and latest onset dates. The spatial pattern of rainy season characteristics are generally consistent with the research of Deng and Wang

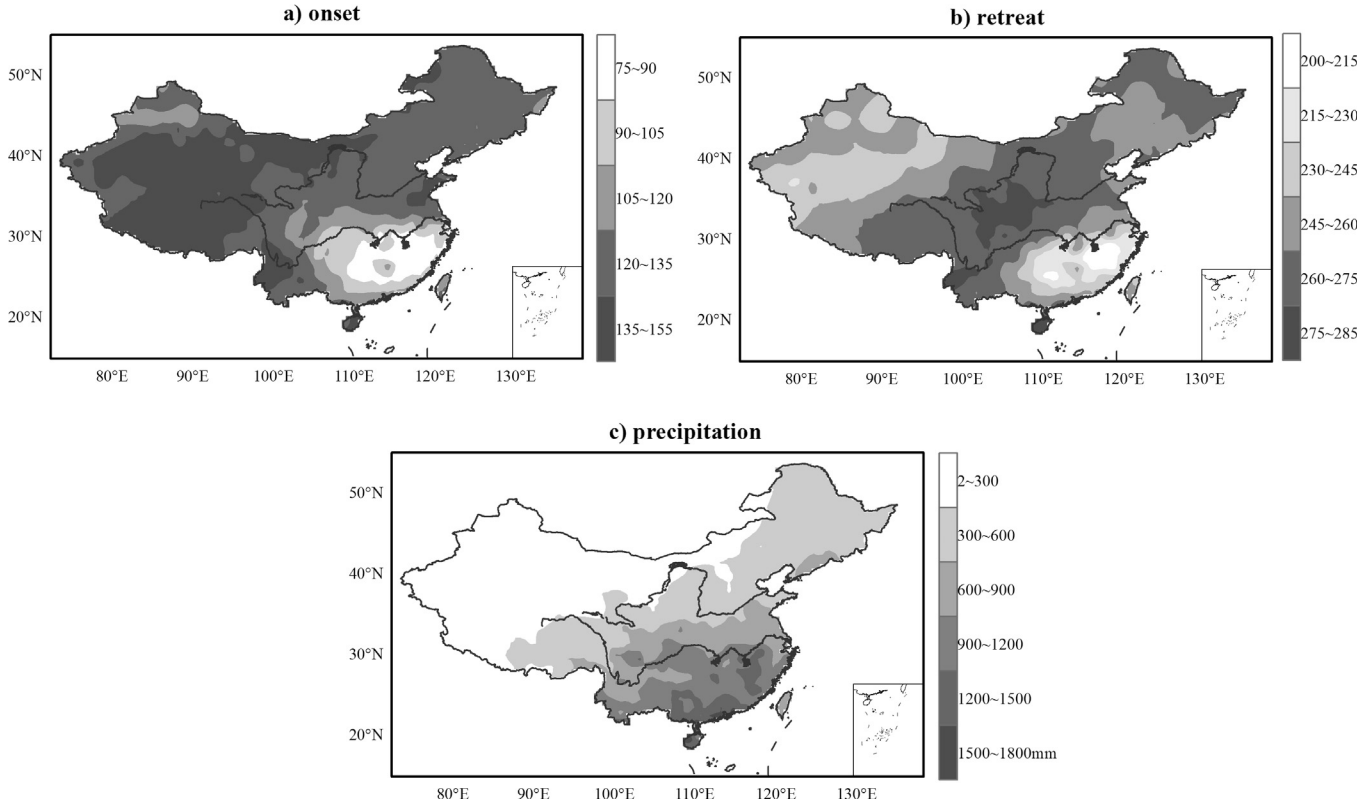

Fig. 3. Spatial patterns of mean values of onset, retreat and precipitation for the period of 1960–2015 in mainland China.

(2002), who argued that rainfall in China mainly occurs in May to July (May–September in the southeastern and southern regions).

It can be seen that the features of rainy season in China vary in space. The regionalization of mainland China, therefore, is necessary in order to describe interannual rainy season characteristics in different regions. K-means clustering method was applied to divide China into sub-regions that have coherent onset, retreat and precipitation features. This classification is based on mean values of multi-year onset, retreat of the rainy season and precipitation during the rainy season. Each station has three parameters (i.e., mean onset, retreat and rainy-season precipitation for the period of 1960–2015), which are used to cluster similar stations. Geographic homogeneity of these stations were also considered in division. Mainland China is divided into five regions (Fig. 4). Region 1 contains mainly the northwestern China and Region 2 includes northeastern China, the Yellow River Basin and northern parts of Huaihe River Basin. Region 3 contains southern regions of the Huaihe River Basin and the northern part of the Yangtze River Basin. Region 4 includes southern regions of the Yangtze River Basin, and Region 5 includes Southeastern China.

The regionalization in Fig. 4 is in accordance with the changing pattern of East Asian Summer Monsoon (EASM) given in Ding and Chan (2005). Zhao et al. (2016) also showed that EASM makes a great contribution to the atmospheric moisture and precipitation in China. Notably, the EASM exhibits some patterns of the onset and retreat. Moreover, rainy season in the mainland China also closely relates to EASM, which will be further presented in Section 4.3.

4.2. Interannual variability

The interannual variability of rainy season is provided in Fig. 5, which displays the time series of average onset, retreat and rainy-season precipitation within the five homogeneous regions from 1960 to 2015. The mean values are determined for each observation station and then averaged for all stations within each region. Pettitt test was applied to detect the abruption point of rainy season characteristics in each region.

In terms of the onset (Fig. 5), there is no evidence of a long-term tendency and no abruption point in Regions 1 for the period of 1960–2015, with the average values of onset Julian day 132. In recent two decades, however, Region 1 displayed obvious delayed trend. Region 2 had a significant mutation point in year 1997 at the level of 0.1. Region 3 had an earlier abruption (year 1979) in comparison with Region 2, before which the onset had a stable level in April. The onset had an advanced trend for the period of 1979–2002, followed by a delayed tendency for 2002–2015.Region 4 displayed similarity to Region 2 with respect to the occurrence time of mutation (Year 1996 in Region 4) and the variation of onset (stabilizing before mutation). The onset in Region 4 had an overall delayed trend for the period of 1960–2015. There is no obvious tendency and no abruption point in Regions 5, with the average values of onset Julian day 107.

The retreat had an abruption point (year 1983) in Region 1, which is statistically significant at the significance level of 5%. The retreat dates advanced approximately a month for 1984–2015 as compared to 1960–1983. Shi et al. (2006) found that the climate change in northwest China is most notably in the year 1987, which is consistent with mutation points detected in this study (year 1983 for retreat and year 1991 for precipitation). It can be seen that the trends of rainy season features in China may be attributed to climate change. Region 2 had the largest variation around the mutation point (year 1976). The fluctuation is gradually shrinking and has a tendency to stabilize at the level of late-September after 1976. Similarly, the retreat fluctuated largely in Region 3 before 2001, followed by decreasing scale of variation. Regions 4 and 5 had no abruption point and no obvious trend of advance or delay.

Precipitation in Region 1 displayed the most distinctive abruption at the year of 1991 and is significant at the level of 1%. After 1991, there is an obvious precipitation increase, with mean values changing from 80 mm to 98 mm per day. Wang et al. (2013) pointed out that daily average precipitation in northwestern China from 1960 to 2009 showed increasing trend, which is consistent with our research. Regions 2–4 had no mutation over 1960–2015 and displayed no apparent tendency. Rainy-season precipitation in Region 5 increased apparently after 1992, with average value of 1390 mm per day, but the trend of precipitation is decreased. Ding et al. (2008) and Wu et al. (2010) revealed that the southern part of China have undergone much more significant rainfall events and 1992 is detected as the climate changing point in the southern China, which is in accordance with our research. Nitta and Hu (1996) and Qian and Qin (2008) also investigated the

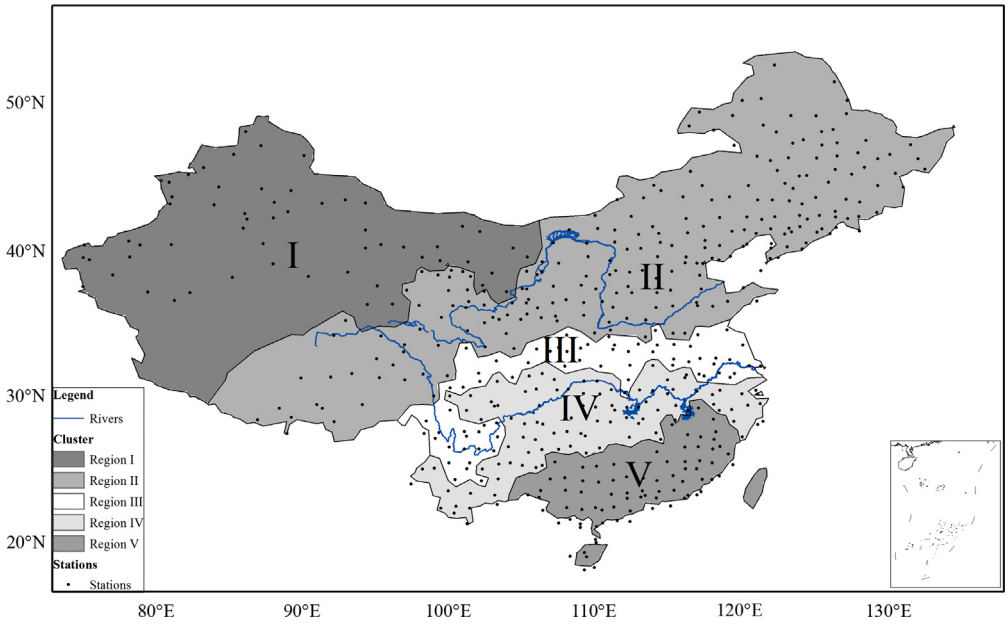

Fig. 4. Regionalization of mainland China based on spatial patterns of onset, retreat and precipitation by cluster analysis.

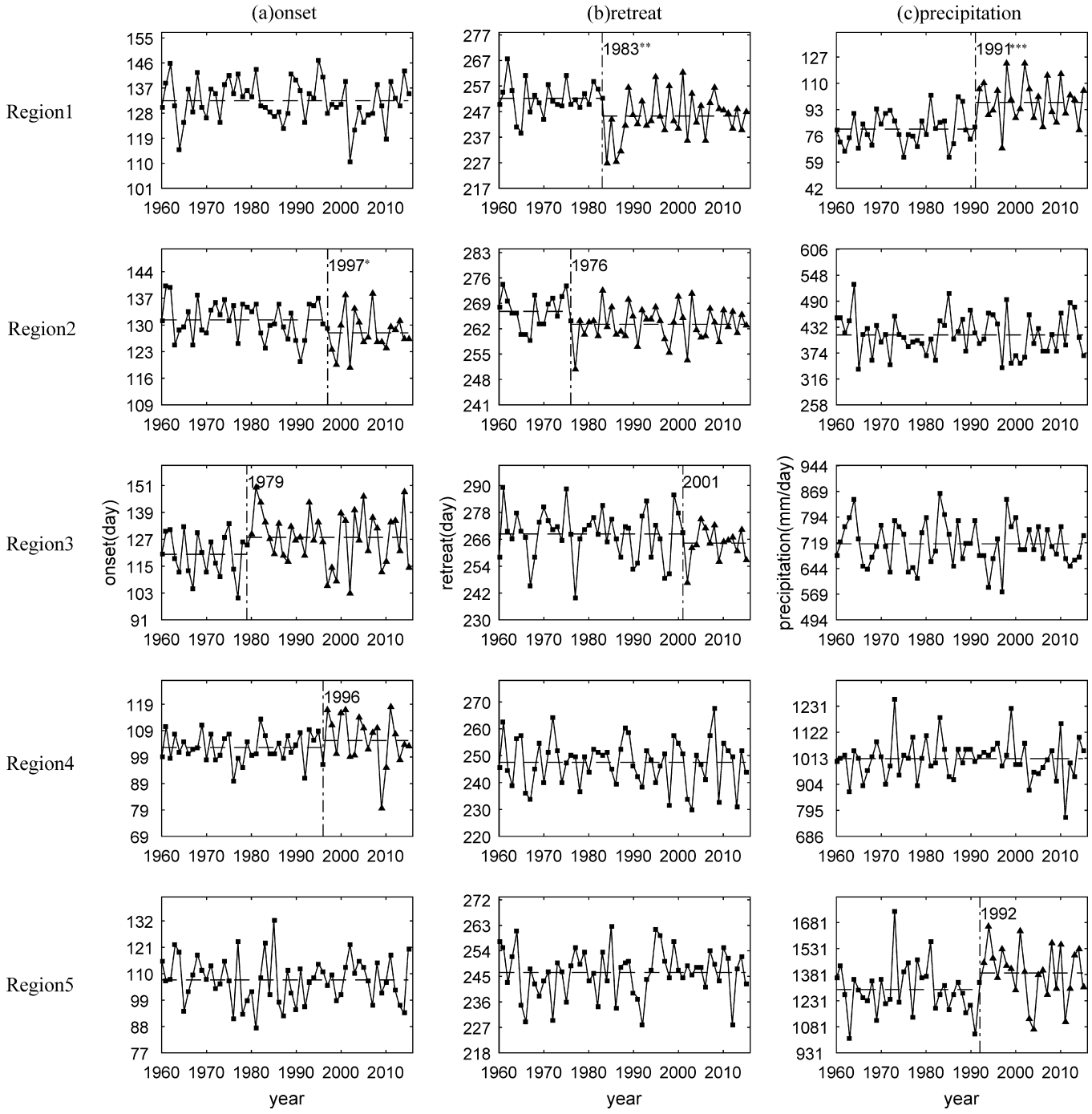

Fig. 5. Interannual variability of rainy season in mainland China. Column (a) represents the interannual variability of onset dates (Julian day) within five regions; Column (b) represents retreat dates (Julian day) and Column (c) rainy-season precipitation (mm). Dashed vertical lines represent the abruption year determined by Pettitt test. * represents the abruption is significant at 0.1 significance level; ** represents the abruption is significant at 0.05 significance level; *** represents the abruption is significant at 0.01 significance level. Dashed horizonal lines are for the avarage onset (a)/retreat (b)/precipitation (c) before and after abruption; if there is no abruption for the period of 1960–2015, dashed horizonal lines are for the avarage onset (a)/retreat (b)/precipitation (c) during 1960–2015.

precipitation division and climate shift in China as well. Their results are different from our research because of the different periods we choose (such as the period of 1960–2000 was chosen in the research of Qian and Qin (2008)) and the different division methods.

In summary, many parts of China displayed delayed onset and advanced retreat at the interannual scale, especially in recent twenty years. Only coastal regions and northwestern China presented increased rainy-season precipitation, with most parts of China had stable precipitation amount. Flooding is more easily trigged under such circumstances, which should be paid enough attention.

4.3. Relationship between rainy season characteristics and atmospheric circulation and SST

4.3.1. Links between the onset and retreat of rainy season and atmospheric circulation

850 hpa vector winds are associated with the moisture transportation from western tropical Pacific to the subtropical region,

which determines the precipitation in China. Marengo et al. (2001) illustrated circulation changes related to the onset and retreat of rainy season in Amazonia by showing composite maps of the difference between the average of 4 pentads after onset/retreat minus the 4 pentads before onset/retreat. 850 hpa vector winds reflecting atmospheric circulation and monsoon variability is used to explore the underlying causes of precipitation variability in this study.

Composite maps of average 850-mb vector winds of 20 days after onset minus 20 days before onset in Region 1 and 4 are shown in Figs. 6 and 7, respectively (the day of onset is not included). Note that composite maps of 850-mb vector winds for the onset in Region 1–3 are similar, with Region 4 similar to Region 5 (not shown). Region 1 and Region 4 are selected to explain the correlation between circulation and the onset in different parts of China. It can be seen from Fig. 6 that, patterns for vector winds are similar before and after onset. The onset of rainy season in Regions 1–3 is associated with an increased cyclone in eastern China and anticyclone near the South China Sea, with an increase composite westerlies from the India Ocean (Fig. 6c). The location of anomalous cyclonic flow for Regions 4–5 is similar to Regions 1–3. The difference between them lies in that the onset of rainy season in Regions 4–5 is mainly controlled by increased cyclone in eastern China rather than the combined influence of anticyclone and cyclone (Fig. 7c). The effect of composite westerlies on Regions 4–5 is also weaker as compared to Regions 1–3.

Regions 1–5 displayed similar patterns regarding the relationship between retreat and monsoon (not shown). Taking Region 1 as the study area, the retreat is influenced by cyclonic flow in the eastern regions of China and anticyclone near the South China Sea as well. However, the retreat is associated with decreased (anti)cyclone and composite easterlies from the South China Sea (Fig. 8).

Figs. 6–8 indicate that the Indian Ocean and the South China Sea are the two principle elements for rainy-season precipitation variability and the onset and retreat of rainy season are associated with (anti)cyclonic flow and monsoon. Wang et al. (2002) found that the spring monsoon precipitation in the southern regions of China is highly related to cyclonic anomalous circulation in the North Pacific, which is consistent with our research. Atmospheric circulation and monsoon are leading drivers determining rainy season features, which is equivalent to the results by Dai and Wigley (2000), Feng et al. (2011), Wu et al. (2003), and Xiao et al. (2015). Previous research found that the beginning of rainy season is also resulted by tropospheric upward motion, upper and low level jet stream and convergence of low-level water vapor over China (e.g., Zhao et al. (2006) and Liu and Ding (2008)). Therefore, it is suggested that more elements should be considered in future research about the physical processes of the onset and retreat of rainy season.

4.3.2. Links between trends of onset, retreat and SST

Table 1 presented various types of ENSO regimes, such as conventional El Niño (CEN) and La Niña (CLN). ENSO Modoki, which is different from conventional ENSO, was introduced by Ashok et al. (2007). ENSO Modoki contains El Niño Modoki (MEN) and La Niña Modoki (MLN). All these regimes play significant roles in the variability of Chinese precipitation (Feng et al., 2010; Wan et al., 2013; Zhou and Chan, 2007). ENSO developing year represents when ENSO occurs, and ENSO decaying year is the following year after ENSO happens. It can be seen from Table 1 that most mutation points of interannual rainy season features (shown in Fig. 5) are associated with ENSO regimes. Yang and Lau (2004) revealed that trends of Chinese precipitation are associated with ENSO-like modes of SSTs, which is in agreement with our research.

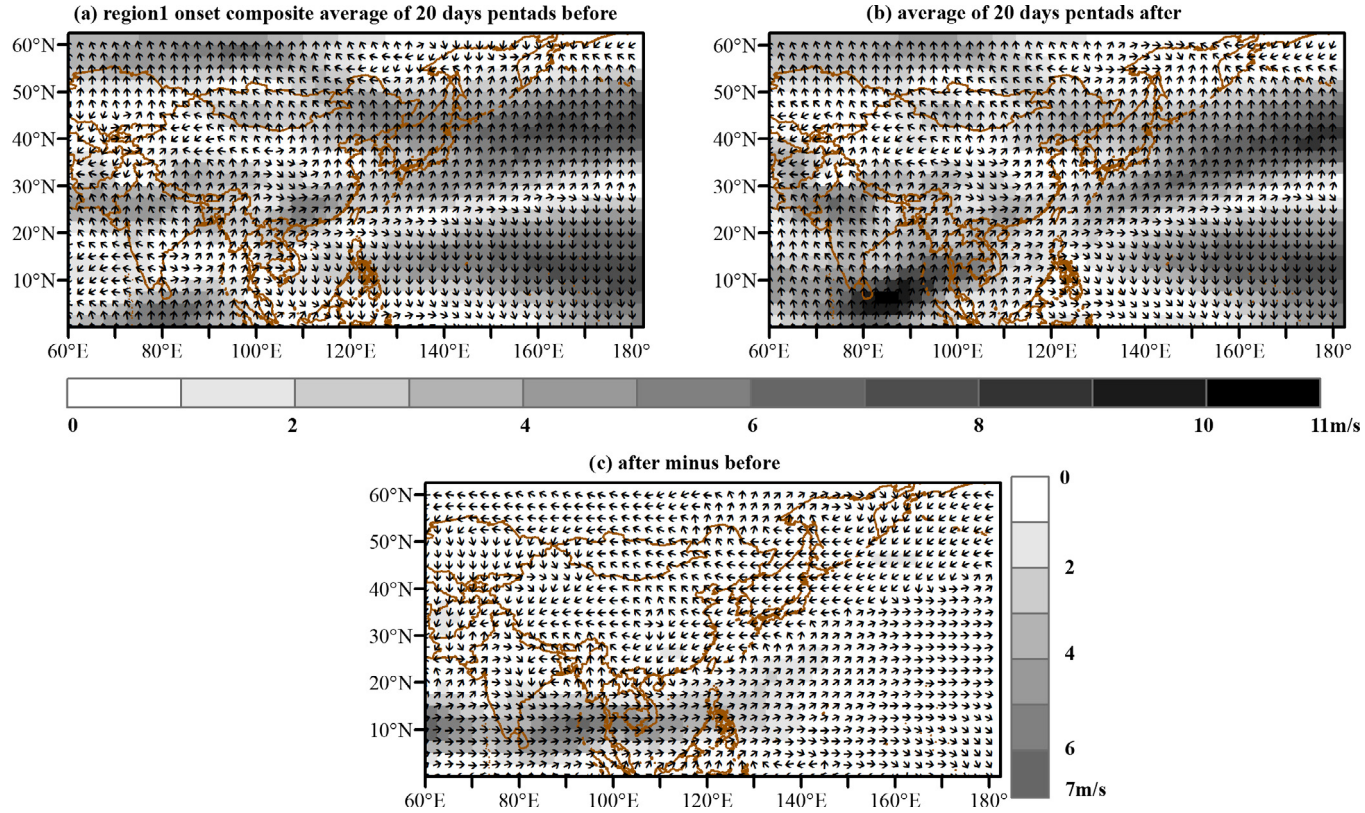

Fig. 6. Composites of 850-mb vector winds for Region 1 (a) average of twenty days before onset; (b) average of twenty days after onset; (c) difference of after (b) minus before (a). Arrows show the direction of wind (m/s); grey shaded areas denote the values of wind speed above 1 m/s.

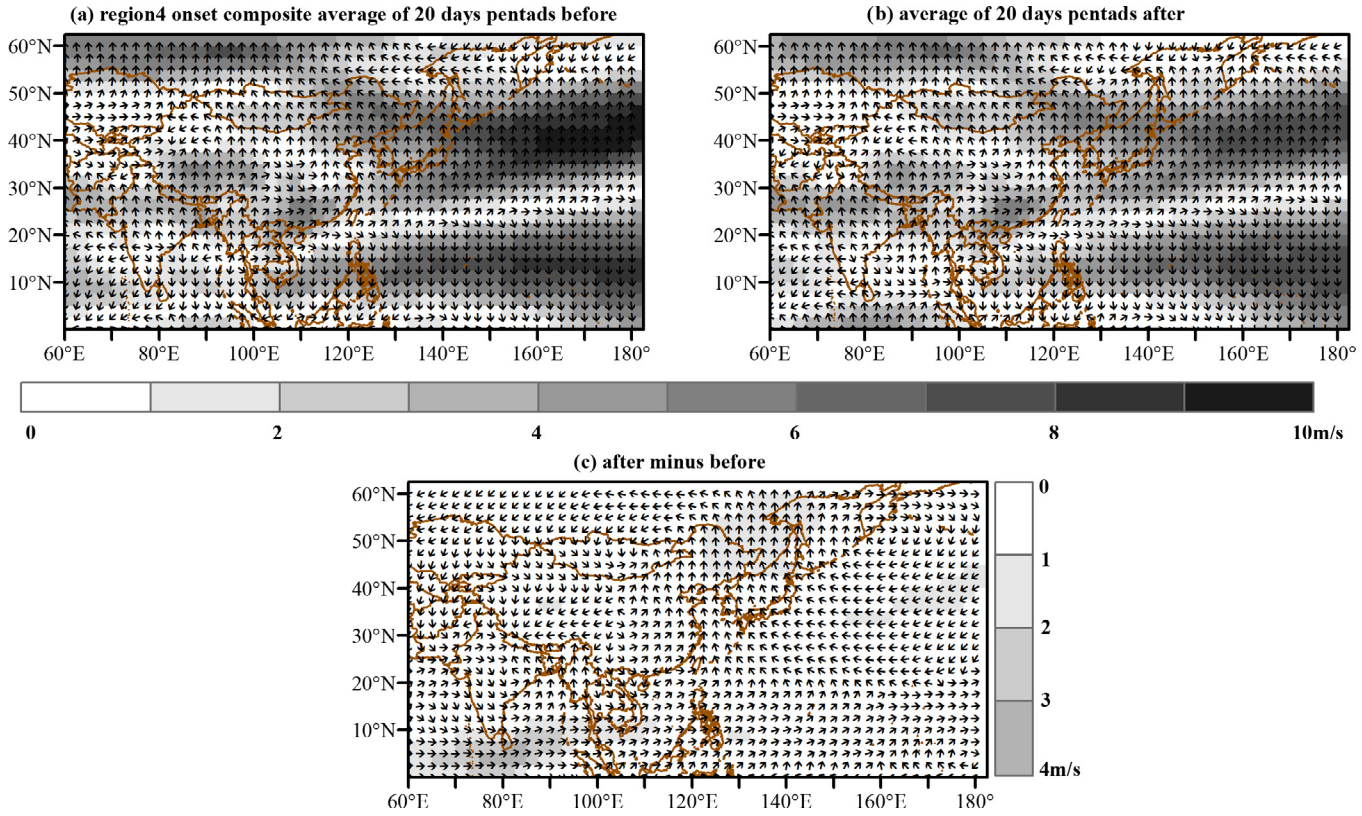

Fig. 7. Composites of 850-mb vector winds for Region 4 (a) average of twenty days before onset; (b) average of twenty days after onset; (c) difference of after (b) minus before (a). Arrows show the direction of wind (m/s); grey shaded areas denote the values of wind speed above 1 m/s.

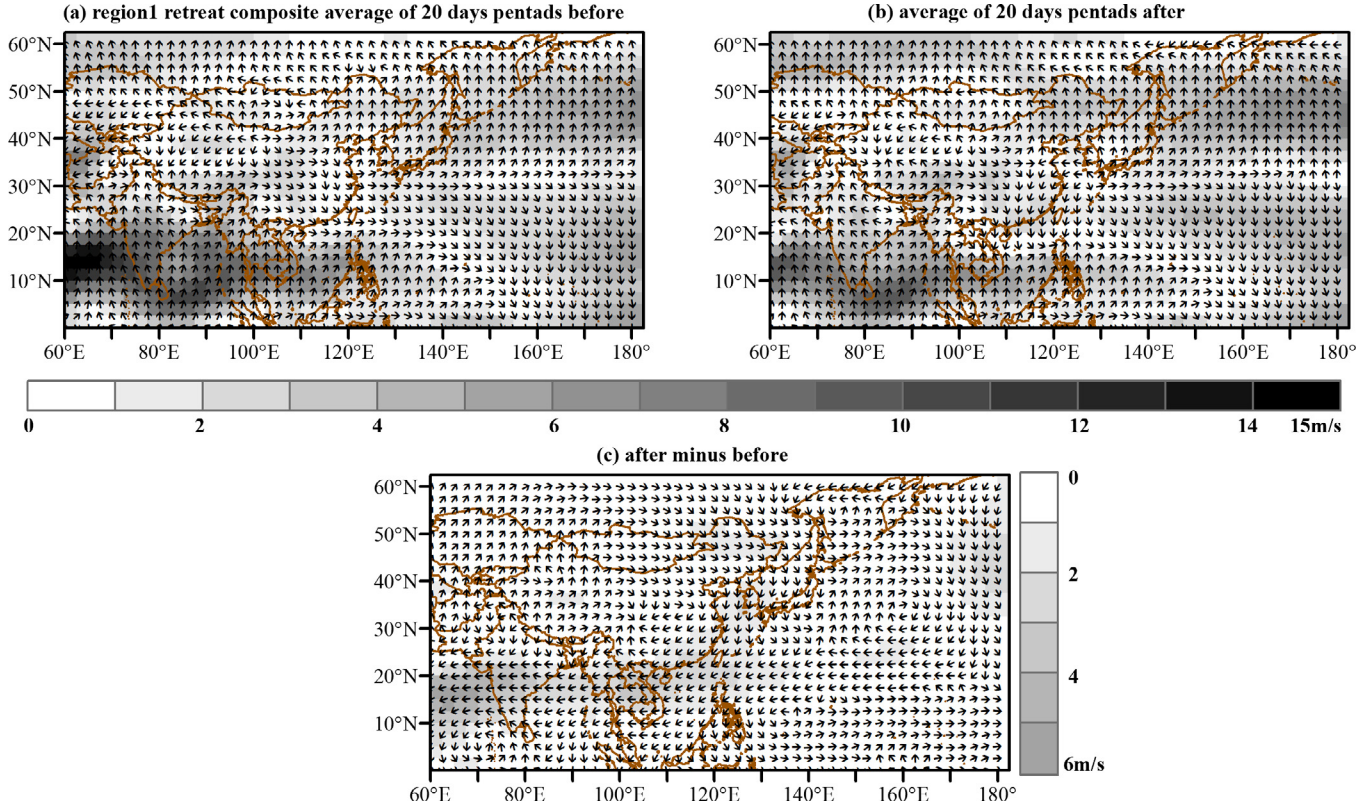

Fig. 8. Composites of 850-mb vector winds for Region 1 (a) average of twenty days before retreat; (b) average of twenty days after retreat; (c) difference of after (b) minus before (a). Arrows show the direction of wind (m/s); grey shaded areas denote the values of wind speed above 1 m/s.

Table 1
Types of abruption year within five regions.

Abruption year	Corresponding to ENSO/normal years
1976	MLN developing year
1979	normal year
1983	CEN developing year
1991	CEN developing year
1992	MEN developing year
1996	normal year
1997	CEN developing year
2001	CLN decaying year

The analysis of SST and onset/retreat within five regions is shown in Figs. 9–13. Correlations between onset/retreat and 3 month average moving values of SST in the preceding periods, with lag ranging from 1 to 12 months, are all investigated in this study. Correlations between preceding SST (lagging 1–12 months) and onset/ retreat are similar (not shown), which suggested that SST and rainy season features displayed stable relationship. Maps are shown below when lag-correlation is strongest among 12 lagged periods.

The onset and retreat in Region 1 all had negative correlation to Pacific SST, indicating that delayed onset and retreat is associated with cold SST (Fig. 9). JJA (June, July, August) SST in eastern and central equatorial Pacific (10°N-20°S, 170°W-100°W) had largest influence on the onset in Region 1 (Fig. 9a). The retreat is best correlated with southern Pacific SST 7 months prior to it (Fig. 9b). Largest correlation between SST and the onset in Region 2 is ASO SST (8 month earlier) in eastern Pacific (20°N-20°S, 140°W-80°W), with SST from October to December prior to retreat having

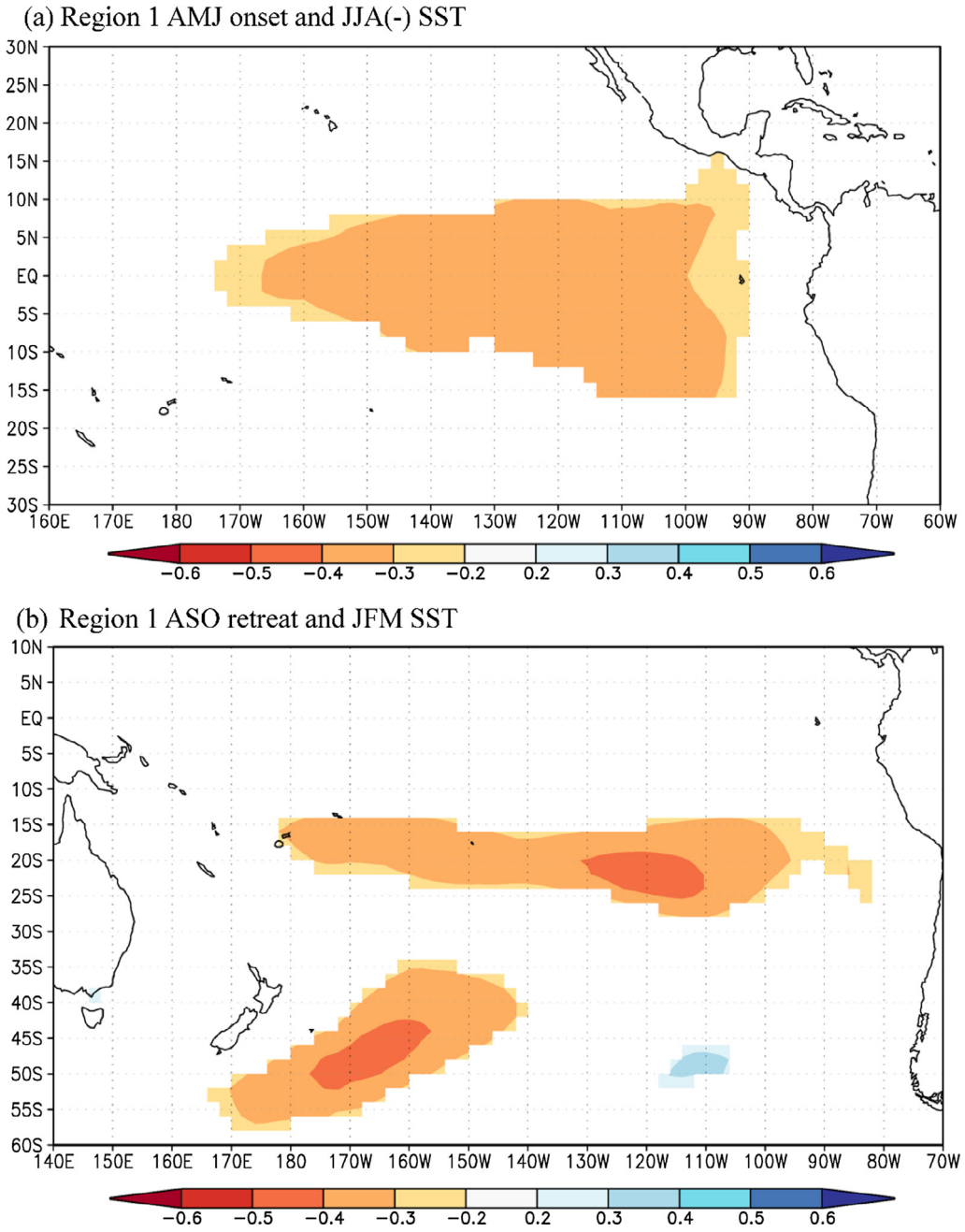

Fig. 9. Correlation between (a) AMJ onset and JJA (–) SST and (b) ASO retreat and JFM SST in Region 1.Shading starts as 0.2, with an interval of 0.1. The "–" within the parenthesis denotes SST in the previous year showing the largest correlation between SST and onset/retreat. They are significant at the 0.05 significance level.

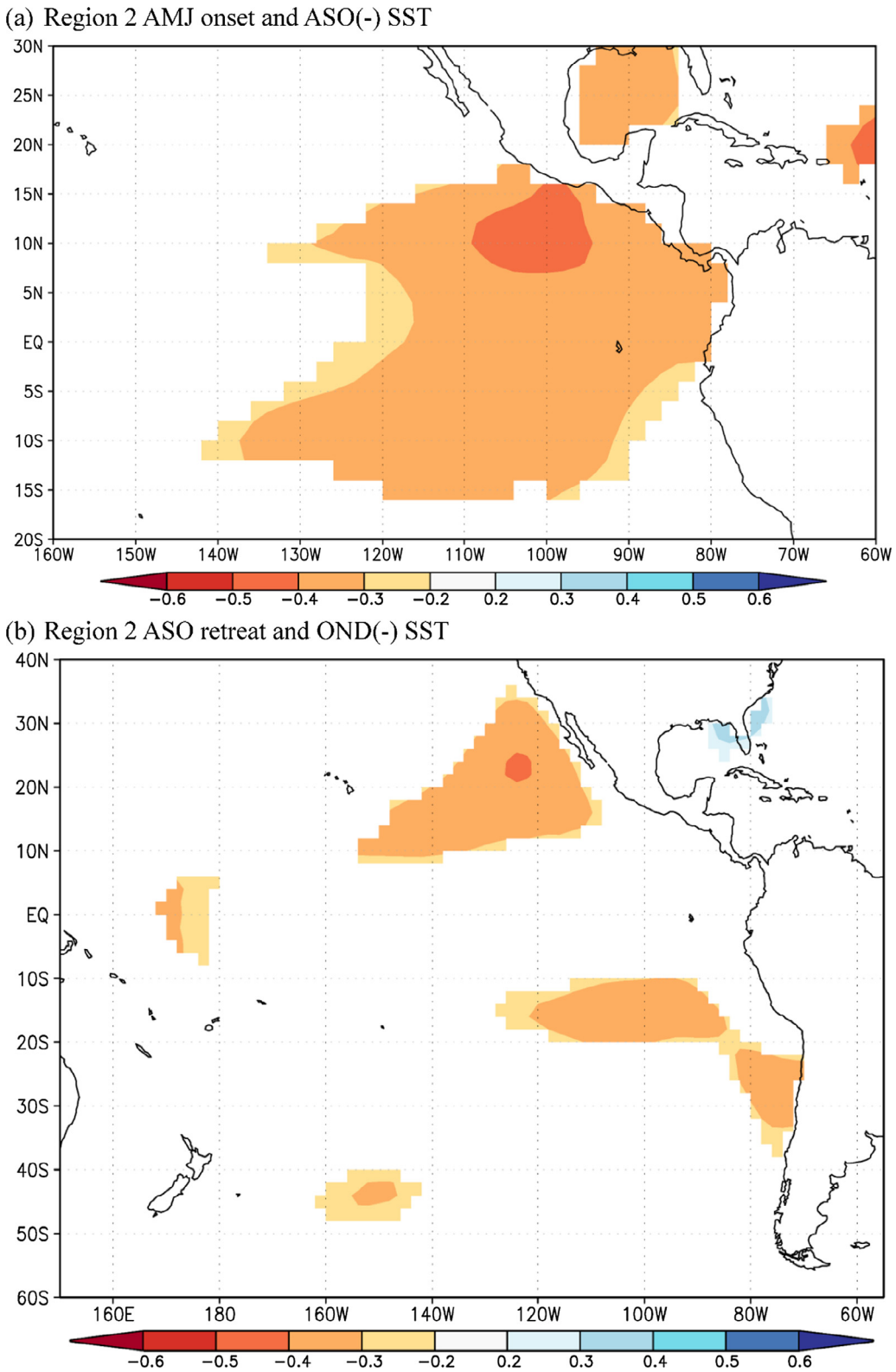

Fig. 10. Correlation between (a) AMJ onset and ASO (−) SST and (b) ASO retreat and OND (−) SST in Region 2. Shading starts as 0.2, with an interval of 0.1. The "−" within the parenthesis denotes SST in the previous year showing the largest correlation between SST and onset/retreat. They are significant at the 0.05 significance level.

strongest relation to retreat (Fig. 10). The extent of SST, showing strong correlation to the onset, is much smaller in Region 3 (6°N-12°S, 115°W-80°W), in comparison to Regions 1 and 2 (Fig. 11a). The retreat showed strong relationship to SST 2 months earlier over large areas of ocean centered on the equatorial Pacific, 150°W (Fig. 11b). Region 4 had the weakest correlation to Pacific SST within five regions (Fig. 12). There is a positive correlation between the South Pacific and the onset in Region 4 and Region 5 (Figs. 12 and 13a), indicating that delayed onset in Region 4–5 is associated with warm SST .

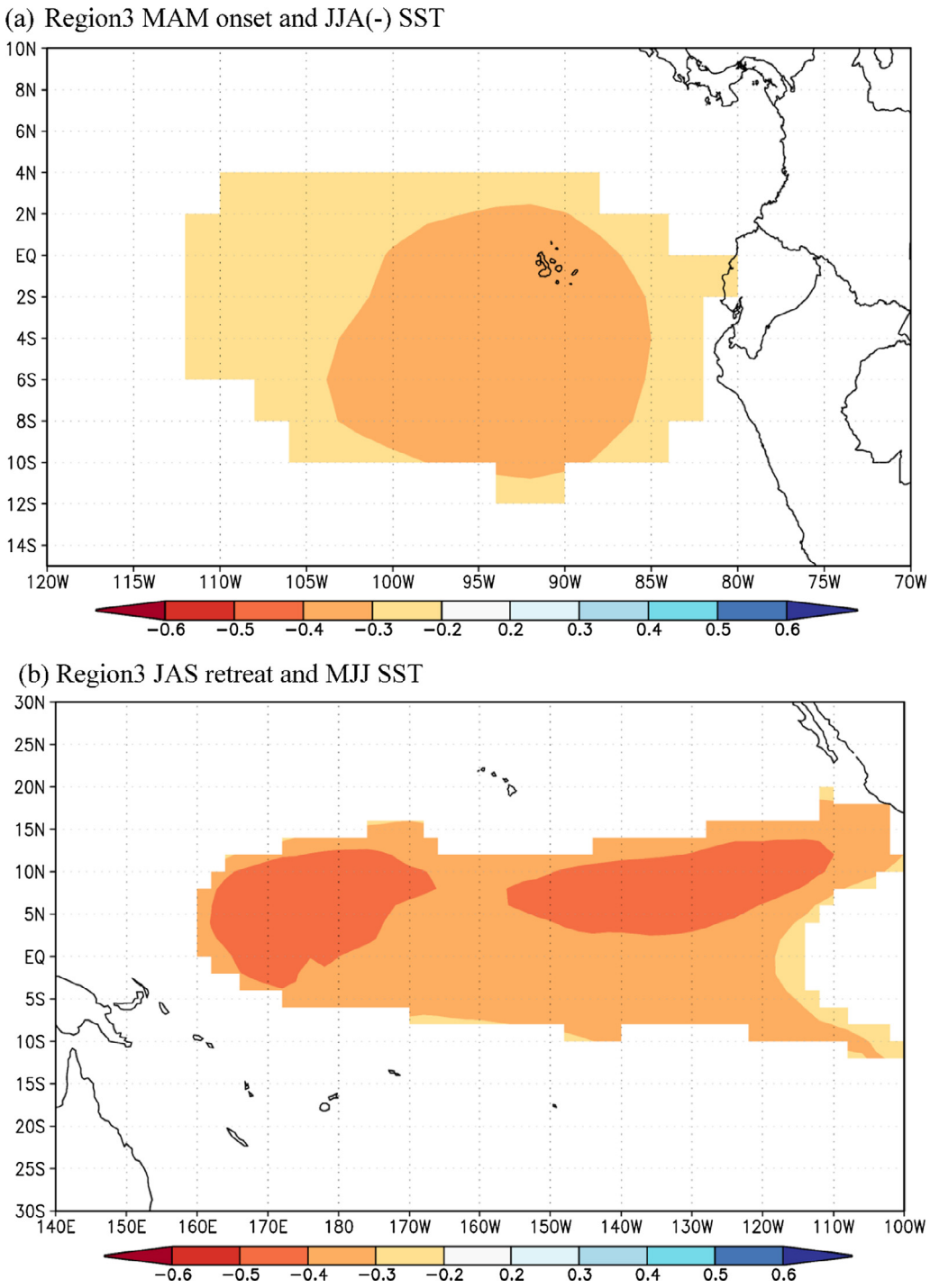

Fig. 11. Correlation between (a) MAM onset and JJA (−) SST and (b) JAS retreat and MJJ SST in Region 3. Shading starts as 0.2, with an interval of 0.1. The "−" within the parenthesis denotes SST in the previous year showing the largest correlation between SST and onset/retreat. They are significant at the 0.05 significance level.

In summary, delayed onset is associated with cold SST in the Pacific Ocean, except in Region 4–5, where delayed onset is caused by warm SST. Advanced retreat in most parts of China may be attributed to warm Pacific SST. SST presenting strong correlation to rainy season characteristics in China is mainly concentrated on Niño regions. This study found rainy season variability is sensitive to ENSO-related SSTs at the interannual scale, which is consistent with the research of Huang and Wu (1989) and Dai and Wigley (2000). Still, the obtained SST correlation may not be physically a cause without analyzing the atmospheric circulation changes that may provide a link. As a consequence, the further exploration of the influence of SST on rainy season in China and their underlying causes, which can be explained by the atmospheric circulation, is presented in the research of Cao et al. (2017). The research reveals that stronger monsoon and anti-cyclone are associated with enhanced rainy-season precipitation under the influence of ENSO. The results also suggest a certain predictability of rainy-season precipitation related to ENSO regimes through the analysis of the atmospheric circulation.

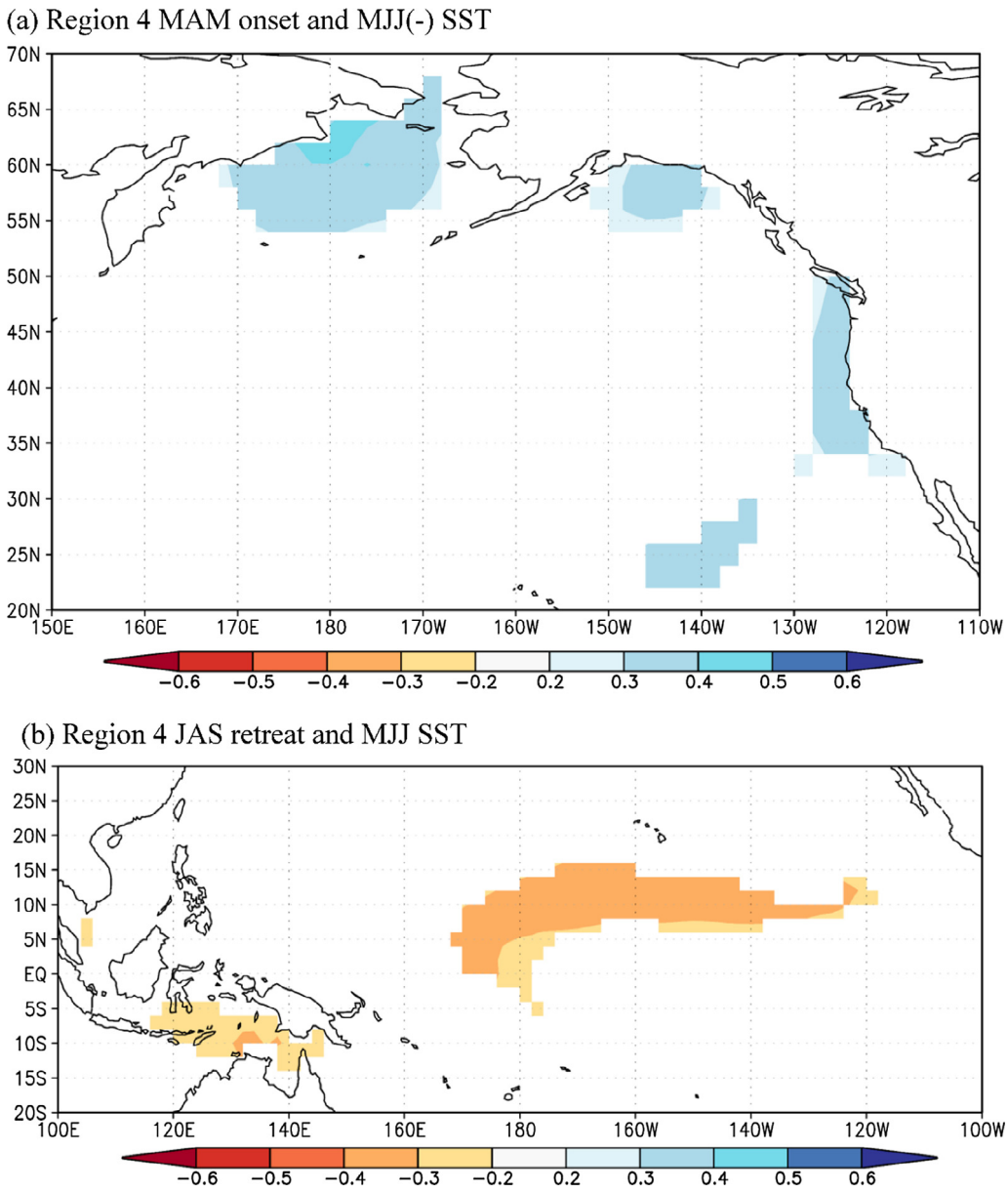

Fig. 12. Correlation between (a) MAM onset and MJJ (−) SST and (b) JAS retreat and MJJ SST in Region 4. Shading starts as 0.2, with an interval of 0.1. The "−" within the parenthesis denotes SST in the previous year showing the largest correlation between SST and onset/retreat. They are significant at the 0.05 significance level.

Different performance of precipitation is associated with the atmospheric circulation and SST, as shown in Sections 4.3.1 and 4.3.2. Previous studies have shown the underlying linkage between monsoon and SST (Black et al., 2003; Chang et al., 2001; Feng et al., 2010; Onyutha and Willems, 2015; Zhang et al., 2014). Wu et al. (2003) explained that the impacts of SST anomalies on precipitation is shown through the physical mechanism of links between SST and the atmospheric circulation. Feng et al. (2011) pointed out that rainfall anomalies in china were mainly because of anomalous anti-cyclone in the western North Pacific related to SST variability. Gerlitz et al. (2016) reported that the change of ENSO-induced precipitation in tropical regions is directly associated with the atmospheric circulation. However, on interdecadal time scales, precipitation patterns are influenced by not only the tropical Pacific SST, but also the subtropical northwestern Pacific high. Besides SSTs, stratosphere–troposphere interactions also play a significant role in rainfall changes in China (Yu et al., 2004). As a result, variability of rainy season features may not only be determined by SST, but also by the combination of various drivers, which ought to be studied further.

5. Conclusions

The onset of rainy season in mainland China started from southeast in middle March to northwest in early June. The occurrence of rainy season is associated with increased anticyclone in South China Sea and cyclone in eastern China. Composite westerlies originate from the India Ocean also plays a significant role on the onset of rainy season. The retreat propagating from southeast (late July) to the central part of China (mid-October) and shrank from the central region to the northwest. The retreat of rainy season is considerably determined by composite easterlies and decreased cyclone and anticylcone. Delayed onset (advanced retreat) are observed in many parts of China at the interannual scale, which is associated with cold (warm) SST in conventional ENSO regions. Enhanced rainy-season precipitation is found in northwestern

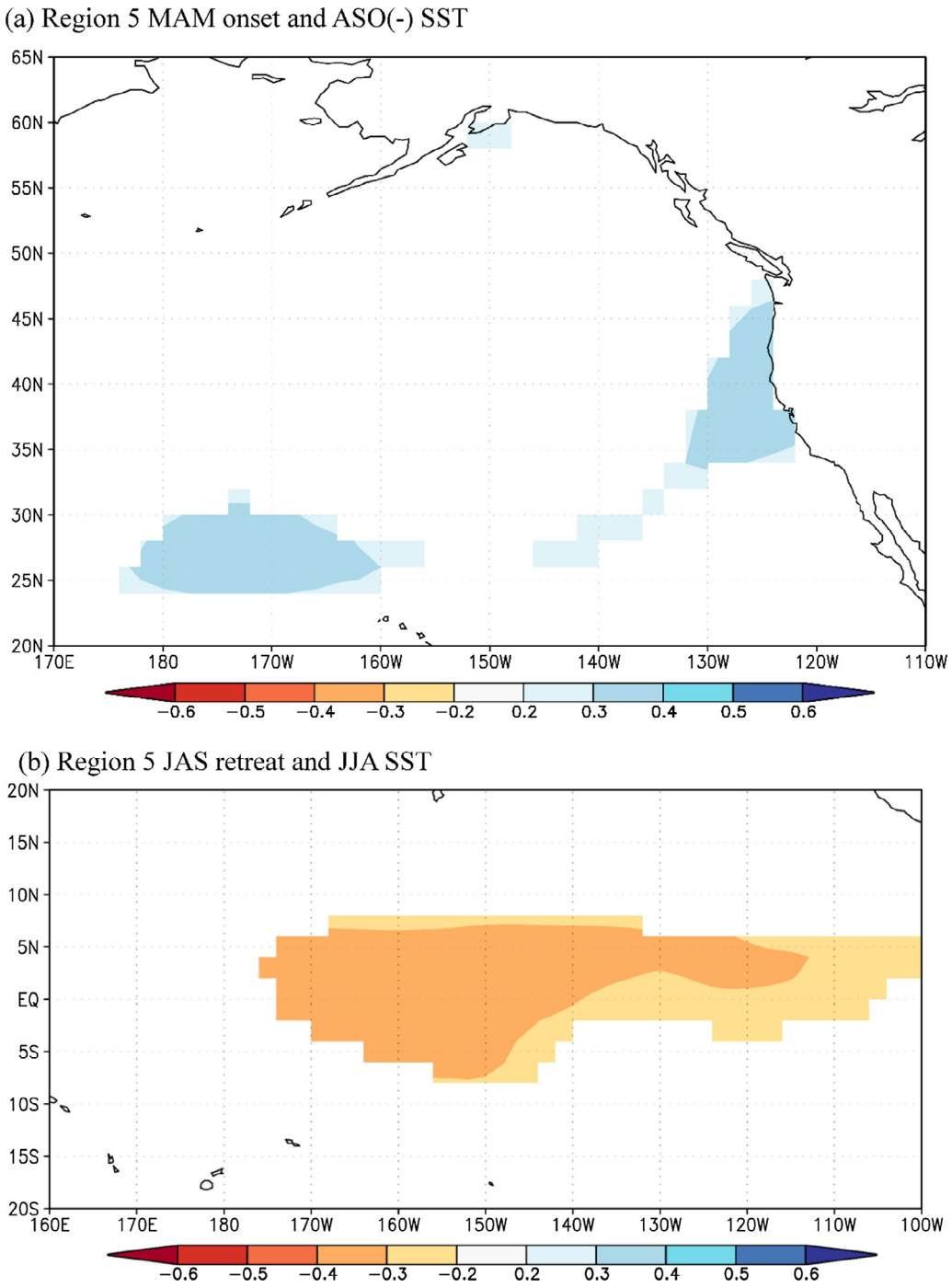

Fig. 13. Correlation between (a) MAM onset and ASO (−) SST and (b) JAS retreat and JJA SST in Region 5. Shading starts as 0.2, with an interval of 0.1. The "−" within the parenthesis denotes SST in the previous year showing the largest correlation between SST and onset/retreat. They are significant at the 0.05 significance level.

and southwestern China, with other regions displaying stable precipitation. Hence, it is easier to trigger flooding under such circumstances, which should be paid enough attention. This study improves our understanding regarding spatial and interannual variability of Chinese rainy season and suggests that there may be certain predictability in Chinese rainy season features related to atmospheric circulation and ENSO-like modes of SSTs.

Author contributions

Quanxi Shao, Qing Cao and Zhenchun Hao conceived the study. All authors contributed to writing the paper.

Competing interests

The authors declare no conflict of interest.

Acknowledgements

This work was supported by the National Key R&D Program of China (Grant No. 2016YFC0402704), the National Natural Science Foundation of China (Grant No. 41371047), the Special Fund of State Key Laboratory of Hydrology-Water Resources and Hydraulic Engineering (Grant No. 1069-514031112) and the CAS-CSIRO Joint Research Program. The authors would like to thank Professor Xun

Sun, East China Normal University, Shanghai, China, for helping us complete this study successfully. The authors would also thank the anonymous reviewers for their constructive comments, which greatly helped improve this paper.

References

Ashok, K., Behera, S.K., Rao, S.A., Weng, H., Yamagata, T., 2007. El Niño Modoki and its possible teleconnection. J. Geophys. Res. Oceans 112 (C11), C11007. https://doi.org/10.1029/2006JC003798.

Ashok, K., Tam, C.Y., Lee, W.J., 2009. ENSO Modoki impact on the Southern Hemisphere storm track activity during extended austral winter. Geophys. Res. Lett. 36 (12), L12705. https://doi.org/10.1029/2009gl038847.

Black, E., Slingo, J., Sperber, K.R., 2003. An observational study of the relationship between excessively strong short rains in coastal East Africa and Indian Ocean SST. Mon. Wea. Rev. 131 (1), 74–94. https://doi.org/10.1175/1520-0493(2003)131<0074:AOSOTR>2.0.CO;2.

Cao, Q., Hao, Z., Yuan, F., Su, Z., Berndtsson, R., Hao, J., Tsring, N., 2017. Impact of ENSO regimes on developing- and decaying-phase precipitation during rainy season in China. HESS 21, 1–12. https://doi.org/10.5194/hess-21-5415-2017.

Chang, C., Harr, P., Ju, J., 2001. Possible roles of Atlantic circulations on the weakening Indian monsoon rainfall–ENSO relationship. J. Climate 14 (11), 2376–2380. https://doi.org/10.1175/1520-0442(2001) 014<2376:PROACO>2.0.CO;2.

Chen, Y., Li, W., Xu, C., Hao, X., 2007. Effects of climate change on water resources in Tarim River Basin. Northwest China. J. Environ. Sci 19 (4), 488–493. https://doi.org/10.1016/s1001-0742(07)60082-5.

Cook, G.D., Heerdegen, R.G., 2001. Spatial variation in the duration of the rainy season in monsoonal Australia. Int. J. Climatol. 21 (14), 1723–1732. https://doi.org/10.1002/joc.704.

Dai, A., Wigley, T.M.L., 2000. Global patterns of ENSO-induced precipitation. Geophys. Res. Lett. 27 (9), 1283–1286. https://doi.org/10.1029/1999gl011140.

Deng, L., Wang, Q., 2002. On the relationship between precipitation anomalies in the first raining season (April–June) in southern China and SST over offshore waters in China. J. Trop. Meteorol. 18 (1), 45–55. 1006-8775(2002) 01-0075-10.

Ding, Y., Chan, J.C.L., 2005. The East Asian summer monsoon: an overview. Meteorol. Atmos. Phys. 89 (1–4), 117–142. https://doi.org/10.1007/s00703-005-0125-z.

Ding, Y., Wang, Z., Sun, Y., 2008. Inter-decadal variation of the summer precipitation in East China and its association with decreasing Asian summer monsoon. Part I: observed evidences. Int. J. Climatol. 28 (9), 1139–1161. https://doi.org/10.1002/joc.1615.

Fan, L., Shin, S.I., Liu, Q., Liu, Z., 2013. Relative importance of tropical SST anomalies in forcing East Asian summer monsoon circulation. Geophys. Res. Lett. 40 (10), 2471–2477. https://doi.org/10.1002/grl.50494.

Feng, J., Wang, L., Chen, W., Fong, S.K., Leong, K.C., 2010. Different impacts of two types of Pacific Ocean warming on Southeast Asian rainfall during boreal winter. J. Geophys. Res. Atmos. 115 (D24), D24122. https://doi.org/10.1029/2010jd014761.

Feng, J., Chen, W., Tam, C.Y., Zhou, W., 2011. Different impacts of El Niño and El Niño Modoki on China rainfall in the decaying phases. Int. J. Climatol. 31 (14), 2091–2101. https://doi.org/10.1002/joc.2217.

Figueroa, S.N., Satyamurty, P., Da Silva Dias, P.L., 1995. Simulations of the summer circulation over the South American region with an eta coordinate model. J. Atmos. Sci. 52 (10), 1573–1584. https://doi.org/10.1175/1520-0469(1995)052<1573:SOTSCO>2.0.CO;2.

Fraedrich, K., Jiang, J., Gerstengarbe, F.W., Werner, P.C., 1997. Multiscale detection of abrupt climate changes: application to River Nile flood levels. Int. J. Climatol. 17 (12), 1301–1315. https://doi.org/10.1002/(SICI)1097-0088(199710)17:12<1301::AID-JOC196>3.0.CO;2-W.

Gan, M., Kousky, V., Ropelewski, C., 2004. The South America monsoon circulation and its relationship to rainfall over west-central Brazil. J. Climate 17 (1), 47–66. https://doi.org/10.1175/1520-0442(2004) 017<0047:TSAMCA>2.0.CO;2.

Gan, M.A., Rao, V.B., Moscati, M.C.L., 2005. South American monsoon indices. Atmos. Sci. Lett. 6 (4), 219–223. https://doi.org/10.1002/asl.119.

Gemmer, M., Fischer, T., Jiang, T., Su, B., Liu, L.L., 2011. Trends in precipitation extremes in the Zhujiang River Basin. South China. J. Climate 24 (3), 750–761. https://doi.org/10.1175/2010jcli3717.1.

Gerlitz, L., Vorogushyn, S., Apel, H., Gafurov, A., Unger-Shayesteh, K., Merz, B., 2016. A statistically based seasonal precipitation forecast model with automatic predictor selection and its application to central and south Asia. Hydrol. Earth Syst. Sci. 20 (11), 4605–4623. https://doi.org/10.5194/hess-20-4605-2016.

Goswami, B., Xavier, P.K., 2005. ENSO control on the South Asian monsoon through the length of the rainy season. Geophys. Res. Lett. 32 (18). https://doi.org/10.1029/2005GL023216.

Huang, R., Wu, Y., 1989. The influence of ENSO on the summer climate change in China and its mechanism. Adv. Atmos. Sci. 6 (1), 21–32. https://doi.org/10.1007/BF02656915.

Jain, A.K., 2010. Data clustering: 50 years beyond K-means. Pattern Recogn Lett 31 (8), 651–666. https://doi.org/10.1016/j.patrec.2009.09.011.

Janowiak, J.E., Xie, P., 2003. A global-scale examination of monsoon-related precipitation. J. Climate 16 (24), 4121–4133. https://doi.org/10.1175/1520-0442(2003) 016<4121:AGEOMP>2.0.CO;2.

Kalnay, E., Kanamitsu, M., Kistler, R., Collins, W., Deaven, D., Gandin, L., Iredell, M., Saha, S., White, G., Woollen, J., Zhu, Y., Leetmaa, A., Reynolds, R., Chelliah, M., Ebisuzaki, W., Higgins, W., Janowiak, J.E., Mo, K.C., Ropelewski, C., Wang, J., Jenne, R., Joseph, D., 1996. The NCEP/NCAR 40-year reanalysis project. Bull. Amer. Meteor. Soc. 77 (3), 437–471. https://doi.org/10.1175/1520-0477(1996)077<0437:TNYRP>2.0.CO;2.

Lenters, J., Cook, K., 1997. On the origin of the Bolivian high and related circulation features of the South American climate. J. Atmos. Sci. 54 (5), 656–678. https://doi.org/10.1175/1520-0469(1997) 054<0656:OTOOTB>2.0.CO;2.

Liebmann, B., Camargo, S.J., Seth, A., Marengo, J.A., Carvalho, L.M.V., Allured, D., Fu, R., Vera, C.S., 2007. Onset and end of the rainy season in South America in observations and the ECHAM 4.5 Atmospheric General Circulation Model. J. Climate 20 (10), 2037–2050. https://doi.org/10.1175/jcli4122.1.

Liebmann, B., Marengo, J., 2001. Interannual variability of the rainy season and rainfall in the Brazilian Amazon Basin. J. Climate 14 (22), 4308–4318. https://doi.org/10.1175/1520-0442(2001) 014<4308:IVOTRS>2.0.CO;2.

Liu, Y., Ding, Y., 2008. Teleconnection between the Indian summer monsoon onset and the Meiyu over the Yangtze River Valley. Sci. China, Ser. D Earth Sci. 51 (7), 1021–1035. https://doi.org/10.1007/s11430-008-0073-9.

Lu, R., 2005. Interannual variation of North China rainfall in rainy season and SSTs in the equatorial eastern Pacific. Chin. Sci. Bull. 50 (18), 2069. https://doi.org/10.1360/04wd0271.

Marengo, J.A., Liebmann, B., Kousky, V.E., Filizola, N.P., Wainer, I.C., 2001. Onset and end of the rainy season in the Brazilian Amazon Basin. J. Climate 14 (5), 833–852. https://doi.org/10.1175/1520-0442(2001) 014<0833:OAEOTR>2.0.CO;2.

Marteau, R., Sultan, B., Moron, V., Alhassane, A., Baron, C., Traoré, S.B., 2011. The onset of the rainy season and farmers' sowing strategy for pearl millet cultivation in Southwest Niger. Agric. Forest Meteorol. 151 (10), 1356–1369. https://doi.org/10.1016/j.agrformet.2011.05.018.

Nitta, T., Hu, Z.-Z., 1996. Summer climate variability in China and its association with 500 hPa height an tropical convection. J. Meteor. Soc. Japan 74 (4), 425–445. https://doi.org/10.2151/jmsj1965.74.4_425.

Omotosho, J.B., Balogun, A., Ogunjobi, K., 2000. Predicting monthly and seasonal rainfall, onset and cessation of the rainy season in West Africa using only surface data. Int. J. Climatol. 20 (8), 865–880. https://doi.org/10.1002/1097-0088(20000630)20:8<865::AID-JOC505>3.0.CO;2-R.

Onyutha, C., Willems, P., 2015. Spatial and temporal variability of rainfall in the Nile Basin. Hydrol. Earth Syst. Sci. 19 (5), 2227–2246. https://doi.org/10.5194/hess-19-2227-2015.

Pearson, K., 1895. Note on regression and inheritance in the case of two parents. Proc. R. Soc. London 58, 240–242.

Pettitt, A., 1979. A non-parametric approach to the change-point problem. Appl. Stat., 126–135

Qian, W., Lee, D.-K., 2000. Seasonal march of Asian summer monsoon. Int. J. Climatol. 20 (11), 1371–1386. https://doi.org/10.1002/1097-0088(200009)20:11<1371::AID-JOC538>3.0.CO;2-V.

Qian, W.H., Qin, A., 2008. Precipitation division and climate shift in China from 1960 to 2000. Theor. Appl. Climatol. 93 (1–2), 1–17. https://doi.org/10.1007/s00704-007-0330-4.

Ratnam, J.V., Behera, S.K., Masumoto, Y., Takahashi, K., Yamagata, T., 2011. Anomalous climatic conditions associated with the El Niño Modoki during boreal winter of 2009. Clim. Dyn. 39 (1–2), 227–238. https://doi.org/10.1007/s00382-011-1108-z.

Reason, C.J.C., Hachigonta, S., Phaladi, R.F., 2005. Interannual variability in rainy season characteristics over the Limpopo region of southern Africa. Int. J. Climatol. 25 (14), 1835–1853. https://doi.org/10.1002/joc.1228.

Shi, Y., Shen, Y., Kang, E., Li, D., Ding, Y., Zhang, G., Hu, R., 2006. Recent and future climate change in Northwest China. Clim. Change 80 (3–4), 379–393. https://doi.org/10.1007/s10584-006-9121-7.

Smith, T.M., Reynolds, R.W., 2004. Improved extended reconstruction of SST (1854–1997). J. Climate 17 (12), 2466–2477. https://doi.org/10.1175/1520-0442(2004)017<2466:IEROS>2.0.CO;2.

Su, B.D., Jiang, T., Jin, W.B., 2005. Recent trends in observed temperature and precipitation extremes in the Yangtze River basin. China. Theor. Appl. Climatol. 83 (1–4), 139–151. https://doi.org/10.1007/s00704-005-0139-y.

Taschetto, A.S., England, M.H., 2009. El Niño Modoki impacts on Australian rainfall. J. Climate 22 (11), 3167–3174. https://doi.org/10.1175/2008jcli2589.1.

Tedeschi, R.G., Cavalcanti, I.F.A., Grimm, A.M., 2013. Influences of two types of ENSO on South American precipitation. Int. J. Climatol. 33 (6), 1382–1400. https://doi.org/10.1002/joc.3519.

Wan, S., Hu, Y., You, Z., Kang, J., Zhu, J., 2013. Extreme monthly precipitation pattern in China and its dependence on Southern Oscillation. Int. J. Climatol. 33 (4), 806–814. https://doi.org/10.1002/joc.3466.

Wang, B., Lin, Ho, 2002. Rainy season of the Asian-Pacific summer monsoon. J. Climate 15 (4), 386–398. https://doi.org/10.1175/1520-0442(2002) 015<0386:RSOTAP>2.0.CO;2.

Wang, H., Xue, F., Zhou, G., 2002. The spring monsoon in South China and its relationship to Large-Scale circulation features. Adv. Atmos. Sci. 19 (4), 651.

Wang, B., Zhang, Y., Lu, M., 2004. Definition of South China Sea monsoon onset and commencement of the East Asia summer monsoon. J. Climate 17 (4), 699–710.

Wang, B., Zhang, M., Wei, J., Wang, S., Li, S., Ma, Q., Li, X., Pan, S., 2013. Changes in extreme events of temperature and precipitation over Xinjiang, northwest China, during 1960–2009. Quatern. Int. 298, 141–151. https://doi.org/10.1016/j.quaint.2012.09.010.

Wu, R., Hu, Z.-Z., Kirtman, B.P., 2003. Evolution of ENSO-related rainfall anomalies in East Asia. J. Climate 16 (22), 3742–3758. https://doi.org/10.1175/1520-0442(2003) 016<3742:EOERAI>2.0.CO;2.

Wu, R.G., Wen, Z.P., Song, Y., Li, Y.Q., 2010. An interdecadal change in Southern China summer rainfall around 1992/93. J. Climate 23 (9), 2389–2403. https://doi.org/10.1175/2009JCLI3336.1.

Xiao, M., Zhang, Q., Singh, V.P., 2015. Influences of ENSO, NAO, IOD and PDO on seasonal precipitation regimes in the Yangtze River basin. China. Int. J. Climatol. 35 (12), 3556–3567. https://doi.org/10.1002/joc.4228.

Yang, F., Lau, K.M., 2004. Trend and variability of China precipitation in spring and summer: linkage to sea-surface temperatures. Int. J. Climatol. 24 (13), 1625–1644. https://doi.org/10.1002/joc.1094.

Yu, R., Wang, B., Zhou, T., 2004. Tropospheric cooling and summer monsoon weakening trend over East Asia. Geophys. Res. Lett. 31 (22). https://doi.org/10.1029/2004GL021270.

Zhang, R., Li, T., Wen, M., Liu, L., 2014. Role of intraseasonal oscillation in asymmetric impacts of El Niño and La Niña on the rainfall over southern China in boreal winter. Clim. Dyn. 45 (3–4), 559–567. https://doi.org/10.1007/s00382-014-2207-4.

Zhang, Q., Xu, C.Y., Becker, S., Zhang, Z.X., Chen, Y.D., Coulibaly, M., 2009. Trends and abrupt changes of precipitation maxima in the Pearl River basin. China. Atmos. Sci. Lett. 10 (2), 132–144. https://doi.org/10.1002/asl.221.

Zhang, Q., Wang, Y., Singh, V.P., Gu, X., Kong, D., Xiao, M., 2016. Impacts of ENSO and ENSO Modoki+A regimes on seasonal precipitation variations and possible underlying causes in the Huai River basin. China. J. Hydrol. 533, 308–319. https://doi.org/10.1016/j.jhydrol.2015.12.003.

Zhao, P., Zhang, R., Liu, J., Zhou, X., He, J., 2006. Onset of southwesterly wind over eastern China and associated atmospheric circulation and rainfall. Clim. Dyn. 28 (7–8), 797–811. https://doi.org/10.1007/s00382-006-0212-y.

Zhao, P., Yang, S., Yu, R., 2010. Long-term changes in rainfall over Eastern China and large-scale atmospheric circulation associated with recent global warming. J. Climate 23 (6), 1544–1562. https://doi.org/10.1175/2009jcli2660.1.

Zhao, T., Zhao, J., Hu, H., Ni, G., 2016. Source of atmospheric moisture and precipitation over China's major river basins. Front. Earth Sci. 10 (1), 159–170. https://doi.org/10.1007/s11707-015-0497-4.

Zhou, W., Chan, J.C., 2007. ENSO and the South China Sea summer monsoon onset. Int. J. Climatol. 27 (2), 157–167. https://doi.org/10.1002/joc.1380.